

Polarization-dependent optical characterization of poly(phenylquinoxaline) thin films

V. Ksianzou, R. K. Velagapudi, B. Grimm, and S. Schrader

Citation: *Journal of Applied Physics* **100**, 063106 (2006); doi: 10.1063/1.2349471

View online: <http://dx.doi.org/10.1063/1.2349471>

View Table of Contents: <http://aip.scitation.org/toc/jap/100/6>

Published by the [American Institute of Physics](#)



Looking for a specific instrument?

Easy access to the latest equipment.
Shop the *Physics Today* Buyer's Guide.

PHYSICS TODAY

lasers imaging
VACUUM EQUIPMENT instrumentation
software cryogenics **MATERIALS**
+ MORE...

Polarization-dependent optical characterization of poly(phenylquinoxaline) thin films

V. Ksianzou, R. K. Velagapudi, B. Grimm, and S. Schrader^{a)}

Faculty of Engineering, Institute of Photonics, Laser and Plasma Technology, University of Applied Sciences Wildau, Bahnhofstrasse, 15745 Wildau, Germany

(Received 2 March 2006; accepted 10 June 2006; published online 25 September 2006)

Linear optical properties of two types of poly(phenylquinoxaline) (PPQ) are studied by multiwavelength prism coupling technique and optical absorption spectroscopy. Surface roughness measurements are done using atomic force microscopy. PPQs form smooth films of high optical quality having refractive indices above 1.7 in the visible and near infrared spectral ranges. Enhanced birefringence of $\Delta n \sim 0.04$ has been observed in both PPQ films prepared by spin coating. Sellmeier coefficients are derived for the wavelength range starting from 0.532 to 1.064 μm for both TE and TM polarizations. Quantum chemical calculations both on the semiempirical and on the *ab initio* level are carried out in order to calculate the first-order molecular polarizability tensors of the polymer repeat units. From the obtained tensor elements, theoretical values for both the average refractive indices and the maximum expectable birefringence are calculated. Based on these values a more detailed interpretation of the experimental findings is carried out. The dispersion of refractive index is quantified by the value of Abbe's constant (ν_d). In our case the value $\nu_d \approx 11$ indicates high dispersion in the visible spectral range. The imaginary part k of the complex refractive index $n^* = n - ik$ reaches values of $k \leq 10^{-3}$ in the wavelength range from 0.5 to 1 μm . © 2006 American Institute of Physics. [DOI: 10.1063/1.2349471]

I. INTRODUCTION

Polymers as basis materials for integrated optics are now extensively used for a broad range of applications including electro-optic modulators, light emitting diodes, and waveguides for optical signal transmission.¹⁻⁴ Polymers are available at low costs, and they are flexible and easily processed compared to inorganic materials and glasses. For application in linear and nonlinear optical devices, they should show an appropriate combination of optical, electrical, mechanical, and thermal properties. Polyphenylquinoxalines (PPQs) combine advantageous features such as high thermal stability including high glass transition temperatures (250–300 °C), high mechanical stability, and ductility.^{1,5-7} They possess excellent film forming properties that minimize fabrication costs and guarantee high optical quality with good transparency as required for low-loss optical waveguide applications. Details about synthesis, and thermal and mechanical properties of polyphenylquinoxalines have been reported by Wrasidlo and Augl⁷ and by other authors.⁸⁻¹⁰ Since the materials are used as thin films, their optical properties are determined, in general, by the thin film geometry and processing techniques. It is, therefore, important to directly examine material parameters of these thin films rather than infer them from bulk measurements.

Since the refractive index is an important parameter for the design of optical devices such as waveguides, electro-optic modulators, and organic light emitting diodes (OLEDs), its value and dispersion should be known precisely for device optimization. In a previous work, ellipsometry has been used to measure thin film parameters of polyparaphenylenevinylene (PPV) and PPQ films in a thickness range of the order of 200 nm.¹¹

In this paper, precise multiwavelength refractive index measurements are carried out on planar waveguides of polyphenylquinoxalines using the prism coupling technique also known as mode-line (or *m*-line) technique. The multiwavelength analysis provides both refractive index dispersion and the birefringence dispersion accurately. This is an advantage compared to the previously reported ellipsometric measurements which suffer from some major disadvantages when used to measure moderate to thick films, such as the ambiguity caused by the incremental nature of the ellipsometer's thickness measurement. The prism coupler, on the other hand, provides a direct and unambiguous measurement and nonincremental thickness and gives direct access to the refractive index for different polarization directions.

The PPQs used here have a high transparency at wavelengths above 500 nm which is evident from the absorption spectra at the visible and near infrared spectral ranges. This makes them promising materials for waveguide applications.

II. EXPERIMENT

We have investigated two types of polyphenylquinoxaline-based polymers, [7,7'-oxybis(2,3-diphenylquinoxaline)] and [7,7'-(2,2-dichloroethene-1,1-diyl)bis(2,3-diphenylquinoxaline)], also named as PPQ2b [Fig. 1(a)] and PPQ3 [Fig. 1(b)], respectively.¹²

Both polymers have been synthesized from aromatic tetraketones and aromatic tetra-amines in cresol by polycondensation reaction towards high molecular mass polymers (180 000–270 000 g mol⁻¹).^{1,13-17} By-products and low-molecular-reaction products of synthesis are eliminated by

^{a)}Electronic mail: schrader@igw.tfh-wildau.edu

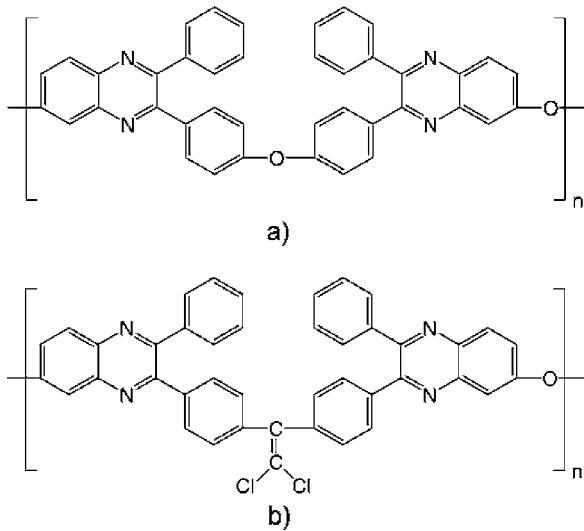


FIG. 1. (a) Chemical structure of 7,7'-oxybis(2,3-diphenylquinoxaline) (PPQ2b) and (b) chemical structure of [7,7'-(2,2-dichloroethene-1,1-diyl)bis(2,3-diphenylquinoxaline) (PPQ3).

repeated precipitation. The molecular structure and purity are verified by NMR spectroscopy, chromatography, UV/vis spectroscopy, and IR spectroscopy. Synthesis is carried out in solvents of spectroscopic purity grade.

PPQ2b and PPQ3 with inherent viscosities $\eta = 1.23$ dl/g and $\eta = 2.3$ dl/g, respectively, were used to form films by solving the polymers in 1,1,2,2-tetrachloroethane (5% by weight). The solubility of the polymers in different solvents was tested and 1,1,2,2-tetrachloroethane was found to be the best. The dissolved polymer was stored in solution at room temperature for about 18 h, avoiding any kind of stirring or shaking of the solution to prevent the formation of microbubbles in the solution. Before film preparation, the polymer solution was filtered through a $0.2 \mu\text{m}$ pore filter. The filtered solution was then deposited onto a substrate of BK7 glass (Melles Griot) precleaned in a 1:3 solution mixture of hydrogen peroxide and sulfuric acid. After rinsing and drying of the substrates the polymer was deposited on them by spin coating with rotation speeds in the range of 700–1200 rpm, producing uniform thin films of thicknesses in the range of 0.8 – $1.85 \mu\text{m}$, depending on viscosity and spin speed. The thin films formed were thermally annealed at 160°C for 1 h to remove any residual solvent. Thin films at low concentrations were also prepared on quartz substrates to obtain the imaginary part of the refractive index by means of absorption measurements.

The optical absorbance spectra of the polymer films with a thickness of 160 nm on quartz substrates in the ultraviolet and visible spectral ranges were measured using a spectrophotometer (Carl Zeiss, Jena, model Specord M 42) at normal incidence. There are two main absorption peaks having their maximum at wavelengths of 376 and 265 nm, which can be assigned to the π - π^* transition of the quinoxaline and the benzene moiety, respectively. In addition, there is a weak absorption around 450 nm connected to the n - π^* transition of the quinoxaline moiety. The thickness of the thin film samples used for absorption measurements is determined by use of a multiangle, single wavelength (632.8 nm) ellipsom-

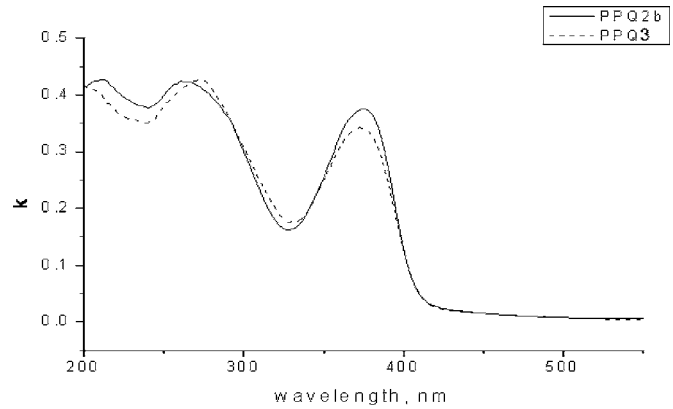


FIG. 2. Imaginary part k of refractive index of PPQ2b and PPQ3 for thin films prepared on quartz glass substrates as deduced from the absorbance spectra. Above 550 nm both materials are transparent ($k \leq 0.001$).

eter (Sentech, model S400). The imaginary part k of the complex refractive index $n^* = n - ik$ of the PPQ samples is calculated from the measured absorbance $A = \log_{10}(I_0/I)$ using the following formula:

$$k = \frac{A\lambda_0}{4\pi d \log_{10} e}, \quad (1)$$

where I_0 and I are the light intensities in front and behind the sample of thickness d and λ_0 is the vacuum wavelength of light for which n and k are determined. A correction of the absorbance spectra with respect to Fresnel reflection losses has not been carried out.

The spectral distributions of k for PPQ2b and PPQ3 obtained from the absorbance spectra according to Eq. (1) are presented in Fig. 2. They show high k values near 0.4 where the absorption peaks of the two polymers occur.

In the present study the m -line technique, which is one of the most precise methods for determining the real part of refractive index, is used. The technique is based on the excitation of TM and TE modes in a planar waveguide and is used for refractive index and thickness measurements of light-guiding films.^{18–20}

Neat PPQ films deposited onto BK7 glass have been measured at various wavelengths starting from 532 up to 1064 nm. In addition, the refractive indices of the substrate (BK7 glass) have also been measured at various wavelengths prior to deposition of the polymer layer in order to compare with the results obtained from the fit to multimode m -line measurements. Good agreement has been found.

The experimental setup of the m -line experiment is shown in Fig. 3(a). The prism-coupler holder is fixed on a motorized two circle goniometer (Huber Diffractionstechnik GmbH, Germany) with a computer-controlled rotation stage, giving the opportunity to change the angle of incidence for the incoming light. The precision of angular position control of the rotation stage is 0.01° . The detector moves around with a double angular speed at an angle 2θ compared to the rotational speed of the sample to detect the reflected beam during the measurements. Mode coupling is realized with the use of high refractive index prism (LaSFN9, Berliner Glass, $n = 1.84489$ at 632.8 nm, $\alpha = 45^\circ$). The detector used is a germanium photodiode (Polytech, Berlin) which is also sen-

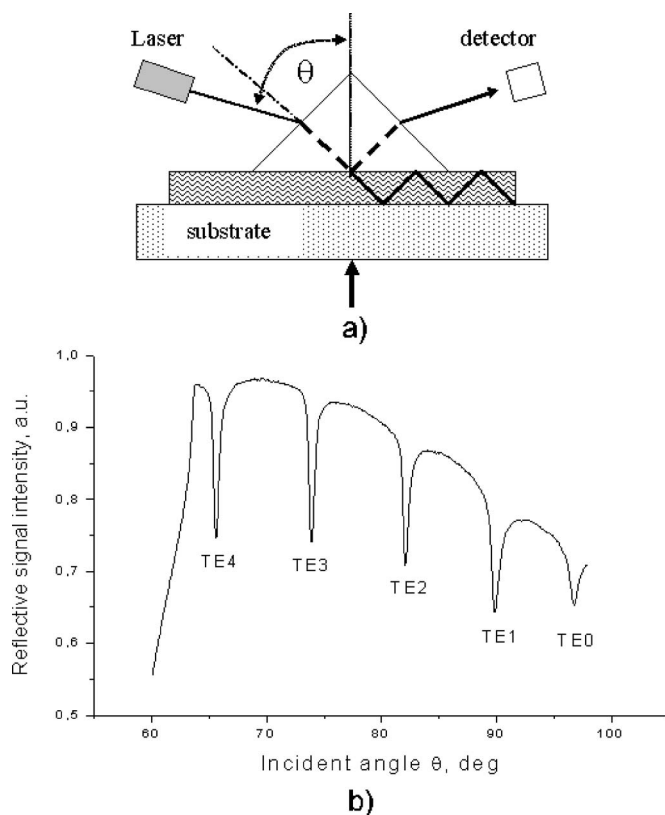


FIG. 3. (a) Setup for *m*-line experiments; (b) pictorial representation of the resulting modes for TE polarization.

sitive in the IR range, i.e., at the telecommunication wavelength regions of 1310 and 1550 nm. A change in the incident light polarization allows the excitation of either the TE or the TM modes. The waveguide modes observed as a set of sharp trenches for the polymer films in a TE polarization state are shown in Fig. 3(b). The prism coupling method based on planar waveguide theory is explained in many sources.^{21,22}

A set of lasers has been used as monochromatic coherent light sources for our study. The wavelengths of 1064 and 532 nm selected are widely considered for use in nonlinear applications as the fundamental and second harmonic wavelengths of the neodymium doped yttrium aluminum garnet (Nd:YAG) laser. The wavelength of 532 nm was generated by a diode pumped Nd:YAG laser with a frequency doubler. The other wavelengths used were 632.8 nm (He-Ne), 980 nm (diode laser, Roithner Laser, Austria), and 1064 nm (diode pumped Nd:YAG laser, Roithner Laser, Austria). Using different but well-defined wavelengths allows us to determine the optical dispersion of the refractive indices with high accuracy.

III. RESULTS AND DISCUSSION

We observed that the solutions of PPQs made in 1,1,2,2-tetrachloroethane (5% by weight) were stable at ambient temperature, which means that the film thickness and its quality are reproducible. Owing to their high glass transition temperatures, PPQs facilitate the use of solvents with high boiling point that are ideal for spin coating for smooth film

formation and annealing at high temperatures. Hence, PPQs are of great interest due to their special properties, including ambient and solution stability.²³ We also observed good hosting capabilities of PPQs with several nonlinear optical chromophores at different doping levels.

The absorption spectra for both the PPQs show two peaks that are similar to each other. The low-energy peak due to the excitons located at the diphenylquinoxaline unit has the same shape and spectral position in both cases. The high-energy peak is slightly redshifted in the case of PPQ3. This might be connected to the influence of the dichloroalkene bridge in PPQ3 replacing one of the two ether bridges prominent in PPQ2b. Film thicknesses measured for PPQ2b and PPQ3 samples used for absorption measurements have been determined by means of ellipsometry, and amount to 150 and 175 nm, respectively. Pure PPQ films are transparent in the region above 450 nm. Due to a slight absorption in the blue part of the spectra, films have a light yellow color.

The choice of solvent is important in connection with surface quality of the films formed from solution. Atomic force microscopy (AFM) measurements on a surface region of dimension of $10 \times 10 \mu\text{m}^2$ of a sample prepared from a polymer-chloroform solution have shown that the film forms an inhomogeneous surface characterized by a so-called orange skin surface pattern due to fast evaporation of chloroform during spin coating. This effect leads to surface discontinuities and hence results in waveguide losses. Tetrachloroethane is used as a solvent in our case that led to more homogeneous films with low roughness. The rms roughness obtained in this case was in the order of 2–3 nm for the films spin coated at various spin speeds and concentrations. The films were smooth as the choice of 1,1,2,2-tetrachloroethane as a solvent has important contribution to this effect due to its high boiling temperatures above 150 °C. Annealing of thin films after spin coating at 160 °C is carried out not only to remove the residual solvent but also to allow the films to rearrange themselves on the substrate. This stabilizes the surface morphology of the films to relax towards a very smooth structure. The optical losses of both PPQ films were measured by monitoring the light scattered out of the waveguide by means of a charge coupled device (CCD) camera, which detects the light along a 2 cm long planar waveguide. The light intensity of scattered light is integrated perpendicular to the propagation direction using 40 lines representing the guided beam and assuming linear intensity dependence of the pixel sensitivity. We derived from that an average loss of 0.8–0.9 dB/cm at 632 nm. The temperature dependence of the optical quality of the thin films is observed by the *in situ* measurements of scattering losses at rising annealing temperature in the range between 50 and 200 °C. We observed a steady decrease of scattering losses upon heating the sample up to 200 °C. Isothermal annealing at 175 °C decreased the scattering losses by about 10% after 2 h. After cooling down to room temperature, the reduced losses are retained, indicating an improved packing of the material.

For the films supporting two or more modes, we obtained both the refractive index and thickness parameters simultaneously (Table I).

Since the *m*-line technique is mode-polarization depen-

TABLE I. Measured mode angles for TE and TM polarizations of PPQ2b and PPQ3 films at various wavelengths.

	Mode 0 (deg)	Mode 1 (deg)	Mode 2 (deg)	Mode 3 (deg)	Mode 4 (deg)	Thickness (μm)	n
PPQ2b							
TE 532 nm	102.93	95.72	86.70	76.95	66.98	1.354	1.778
TM 532 nm	88.78	83.97	77.10	69.14		1.392	1.719
TE 632.8 nm	94.97	87.53	77.80	67.27		1.351	1.741
TM 632.8 nm	84.71	78.82	70.69			1.388	1.688
TE 980 nm	87.12	75.36				1.341	1.700
TM 980 nm	79.48	69.21				1.368	1.655
TE 1064 nm	86.21	73.43				1.346	1.697
TM 1064 nm	78.72	67.60				1.371	1.652
PPQ3							
TE 532 nm	101.17	94.02	84.96	75.09	65.11	1.312	1.773
TM 532 nm	91.17	85.70	78.13	69.50		1.345	1.731
TE 632.8 nm	93.93	86.37	76.48	65.86		1.312	1.737
TM 632.8 nm	86.59	80.05	71.25	75.09		1.344	1.700
TE 980 nm	86.34	74.44				1.310	1.697
TM 980 nm	80.78	69.76				1.337	1.666
TE 1064 nm	85.35	72.37				1.307	1.693
TM 1064 nm	79.83	67.92				1.334	1.662

dent, it allows the determination of birefringence in thin films (which requires waveguide modes to exist for both polarizations). The prism coupling method is based on planar waveguide theory, where the propagation of modes inside the polymer layer can be described by the following equation:

$$\arctan \zeta_{21} + \arctan \zeta_{23} + m\pi = k_{y2}d, \quad (2)$$

where $k_{y,j} = n_j k_0 \sin \theta$ is the y component of the propagation vector of light in the j th layer with the vacuum propagation vector $k_0 = 2\pi/\lambda_0$, the vacuum wave length λ_0 , and the bouncing angle θ which spans the angle between the propagation vector of the reflected wave and the interface between core and cladding. Note that the y direction is perpendicular to the z direction which represents the effective propagation direction of light along the waveguide. The quantities ζ_{ij} are defined as $\zeta_{ij} = \kappa_j / \tau_i$ for TE modes and $\zeta_{ij} = (\varepsilon_i / \varepsilon_j)(\kappa_j / \tau_i)$ for TM modes, with the optical dielectric constant $\varepsilon_j = n_j^2$ of the j th layer. The indices i and j can run from 1 to 3. Here $j = 1$ stands for the substrate, $i = 2$ describes the core, and $j = 3$ represents the upper cladding (superstrate) of the waveguide. The quantities κ_j and τ_j are defined as $\kappa_j = \sqrt{n_{\text{eff}}^2 - n_j^2}$ and $\tau_j = \sqrt{n_j^2 - n_{\text{eff}}^2}$, respectively, where n_j is the refractive index of the j th layer and $n_{\text{eff}} = n_2 \cos \theta$ is the effective refractive index of the core layer ($i = 2$). m represents the order of the waveguide mode. A detailed description of the theory is given in many sources.^{21,22}

The thickness obtained directly from the prism coupling measurements is used in conjunction with the optical absorbance spectra to calculate the imaginary part k of refractive index (extinction coefficient). Although the precision of refractive index measurements is up to 10^{-5} , the pressure applied at the coupling point leads to a deviation of the local refractive index due to a change in density at this point.²⁴ The deviation is of the order of 10^{-4} and depends on the

viscoelastic properties of the polymer.²⁵ Shorter wavelengths can support higher numbers of modes than the longer ones.

Precisely measured values of refractive indices are given in Table II. They have been used to find fit coefficients (see Table II) which describe the dispersion of the real part $n(\lambda)$ of refractive index. A very precise way to describe dispersion of n is based on the well-known Sellmeier formula

$$n^2(\lambda) = 1 + \sum_{i=1}^n \frac{A_i \lambda^2}{\lambda^2 - B_i}. \quad (3)$$

In the present case, according to Ref. 22 a sufficient accuracy has been achieved by means of the following simplified dispersion formula:

$$n^2(\lambda) = n_\infty^2 + \frac{q}{\lambda^2 - \lambda_0^2}. \quad (4)$$

Formally, Eq. (4) can be derived from Eq. (3) by setting $A_i = 0$ for $i \geq 3$, $B_1 = B_3 = 0$, $A_3 = -A_2$, $1 + A_1 = n_\infty^2$, $B_2 = \lambda_0^2$, and $A_2 B_2 = q$. The quantity n_∞ represents the limiting value of refractive index at infinite wavelength and λ_0 the wavelength at resonance. In the approximation of Eq. (4) only one resonance is taken into account. From Table II the following fit parameters as given in Table III have been extracted

TABLE II. Measured refractive indices of PPQ2b and PPQ3 at four different wavelengths for TE and TM polarizations.

Material	532 nm (green)	632.8 nm (red)	980 nm (IR)	1064 nm (IR)
PPQ2b TE	1.778	1.741	1.700	1.697
PPQ2b TM	1.719	1.688	1.655	1.652
PPQ3 TE	1.773	1.737	1.697	1.693
PPQ3 TM	1.731	1.700	1.666	1.662

TABLE III. Fit parameters to Eq. (4) for a PPQ2b and a PPQ3 film of thickness $1.3 \mu\text{m}$ for TE and TM polarizations.

Material	n_∞	λ_0 (μm)	q (μm^2)	ν_d
PPQ2b TE	1.6783	0.306	0.0653	10.1
PPQ2b TM	1.6367	0.294	0.0540	11.8
PPQ3 TE	1.6747	0.295	0.0662	10.6
PPQ3 TM	1.6452	0.286	0.0585	11.6

Since the three-parameter dispersion function of Eq. (4) fits well to the four experimental points, it is proven that the chosen model is adequate to calculate the refractive indices in the transparency region. The precision of the values obtained from Eq. (4) is better than 0.001. In the case of more than four experimental values of refractive index, the measured accuracy of the fit can be enhanced by using Eq. (3) instead of Eq. (4). The fitted values for the wavelength λ_0 are situated in the range between 286 and 306 nm, and correspond to the resonance we assign to the π - π^* transition of the benzene moiety.

The dispersion curves of refractive indices for the thin films of PPQ2b and PPQ3 fitted by means of Eq. (4) are shown in Figs. 4(a) and 4(b), respectively. The refractive index for TE polarization decreases from values near 1.8 to values below 1.7 for both polymers by going from the blue to the Near infrared (NIR) spectral range. In the case of TM polarization, the refractive index decreases from about 1.73 to 1.66 for both polymers in the same spectral region.

A quantitative measure of refractive index dispersion of transparent materials is the Abbe number ν_d , defined by

$$\nu_d = \frac{n_d - 1}{n_F - n_C}, \quad (5)$$

with n_d , n_F , and n_C the refractive indices at three standard wavelengths (yellow helium d line at $0.58756 \mu\text{m}$, blue hydrogen F line at $0.48613 \mu\text{m}$, and red hydrogen C line at $0.65627 \mu\text{m}$, respectively). Both polymers reveal similar values of dispersion for identical polarization, i.e., for TE or TM polarization, respectively, as can be seen in Table III. However, at TM polarization the dispersion is slightly weaker than for TE polarization (the higher ν_d value corresponds to a lower dispersion). The absolute values of Abbe's number of the polymers PPQ2b and PPQ3 in the range between 10 and 12 indicate a relatively high dispersion. Typical values for optical crown glasses, which show low dispersion, are in the range of $\nu_d > 50$.

High birefringence Δn is observed in thin films of both polymers (see Fig. 5). It is calculated as the difference between the refractive indices for TE and TM polarizations. The occurrence of birefringence can be explained by the action of hydrodynamic forces during spin coating, which align the PPQ chains along the rotational plane.¹¹

In order to understand the measured anisotropy of refractive indices, quantum chemical calculations on semiempirical and *ab initio* levels are carried out with the aim to estimate the molecular polarizability tensor of the polymer repeat unit. From the absorption spectra of the polymers with their maxima below 400 nm it can be assumed that the av-

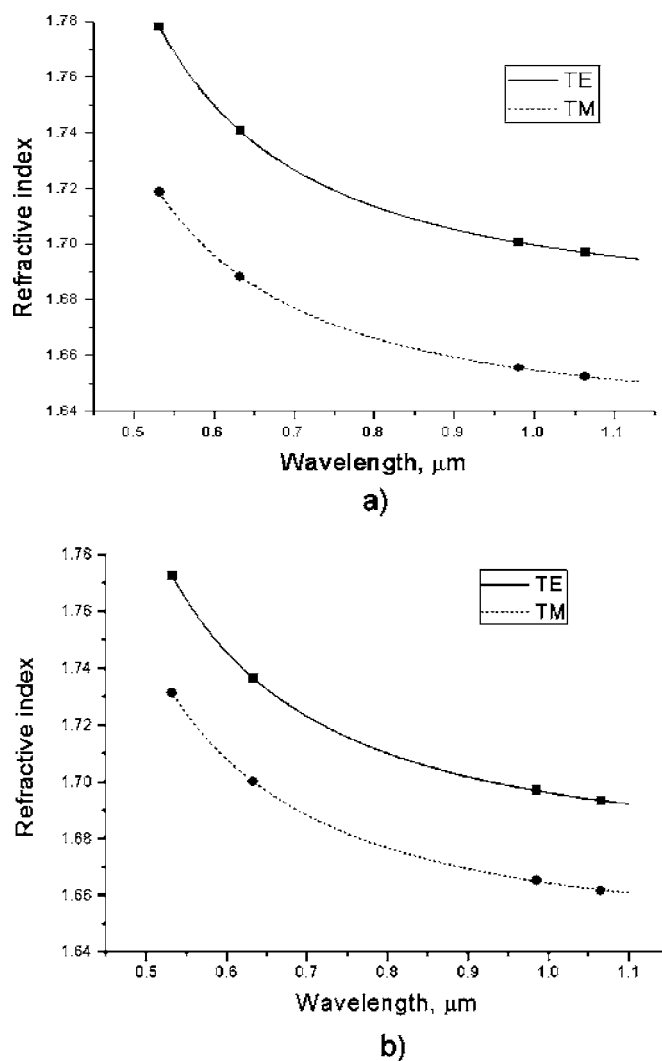


FIG. 4. Dispersion curves as obtained by multiwavelength measurements of refractive index for TE and TM polarizations in the cases of (a) PPQ2b and (b) PPQ3.

erage size of the active chromophore is that of the diphenylquinoxaline moiety. Conjugation is broken by the single bonds of the oxygen or the ethylene dichloride bridge, respectively, which are prominent along the polymer main chain. Consequently, main features concerning absorption and refraction can already be derived from the properties of a single repeat unit. The shape of a repeat unit of PPQ2b optimized by quantum chemical calculations is shown in Fig. 6. For the sake of simplicity, the repeat unit does not contain that oxygen bridge which forms the link to the next repeat unit in the polymer chain. In spite of this simplification, we obtained realistic values for the molecular polarizability tensor elements from which the average refractive indices of the material are calculated. The molecular coordinate system of a repeat unit of PPQ2b as used for the quantum chemical calculations is also shown in Fig. 6.

Combining the Lorenz approximation of a spherical cavity and the Maxwell equations, one obtains the so-called Lorentz-Lorenz equation which combines refractive index n of a homogeneous medium with the ratio $P = \alpha/V$ representing the molecular polarizability α normalized to the molecular volume V according to the following equation:

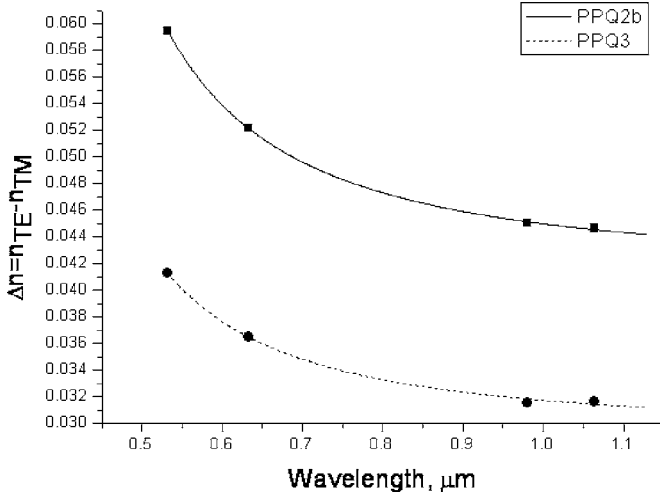


FIG. 5. Birefringence measured in 1.3 μm thick films of PPQ2b and PPQ3. Measured values of PPQ2b and PPQ3 are plotted by squares and circles, respectively.

$$\frac{n^2 - 1}{n^2 + 2} = \frac{4}{3} \pi P \quad (\text{cgs system}), \quad (6)$$

$$\frac{n^2 - 1}{n^2 + 2} = \frac{1}{3\epsilon_a} P \quad (\text{SI system}),$$

where ϵ_a is the dielectric constant of the vacuum: $\epsilon_a = 8.854 \times 10^{-12} \text{ A s/V m}$. The specific polarizability P can be expressed for the given polymers as polarizability α_{unit} of one structural repeat unit per its volume V_{unit} ,

$$P = \frac{\alpha_{\text{unit}}}{V_{\text{unit}}}. \quad (7)$$

This equation holds good for both the cgs and the SI system. The polarizability α has in the cgs system the unit \AA^3 and in the SI system the unit $\text{A s m}^2/\text{V}$, i.e. induced dipole moment per unit field strength. According to Eq. (6), the polarizability α_{cgs} of the cgs system is connected to the polarizability α_{SI} of the SI system via the relation

$$\alpha_{\text{SI}} = 4\pi\epsilon_a\alpha_{\text{cgs}}. \quad (8)$$

The volume V_{unit} of one repeat unit can be found according to Eq. (9) from the density ρ , the molar mass M , and Avogadro's number N_A ,

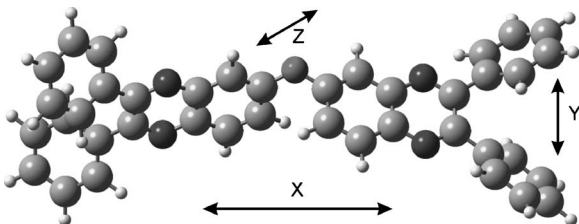


FIG. 6. Optimized structure of the repeat unit of PPQ2b without oxygen bridge forming the link to the next repeat unit. Inertial axes are also shown. The z axis is orthogonal to the plane.

TABLE IV. Principal polarizabilities of PPQ2b and PPQ3 repeat units in cgs units calculated by applying the HF/3-21G+ level of theory together with the corresponding values of refractive index and maximum birefringence.

	α_{xx} (\AA^3)	α_{yy} (\AA^3)	α_{zz} (\AA^3)	α_{unit} (\AA^3)	$\Delta\alpha_{\text{unit}}$ (\AA^3)	n	Δn
PPQ2b	110.54	56.48	50.44	72.49	57.08	1.713	0.731
PPQ3	110.21	65.73	59.68	78.54	47.51	1.670	0.517

$$V_{\text{unit}} = \frac{M}{\rho N_A}. \quad (9)$$

With a measured density of 1.24 g/cm^3 and with average molar masses of the considered repeat units of $M = 578.66 \text{ g/mol}$ for PPQ2B and of $M = 657.59 \text{ g/mol}$ for PPQ3 one obtains molecular volumes V_{unit} per repeat unit of 774.93 and 880.63 \AA^3 , respectively. These numbers do not consider the oxygen bridge, which is linking two adjacent repeat units because for the sake of simplicity it was not included into the quantum chemical calculations.

The theoretical average repeat unit polarizability α_{unit} is obtained by averaging over all the three diagonal components of the calculated polarizability tensor,

$$\alpha_{\text{unit}} = \frac{\alpha_{xx} + \alpha_{yy} + \alpha_{zz}}{3}. \quad (10)$$

We calculated the components of the polarizability tensor for one repeat unit of the polymer chain as shown in Fig. 6. This unit repeats along the polymer chain. These units are connected by ether bridges which provide good solubility and processability of the polymer. In Table IV are the results of quantum chemical analysis applying the Hartree-Fock level of approximation. Since quantum chemical calculations are very time and resource consuming, we performed a pre-analysis of smaller structural parts of PPQ units at different arbitrary basis sets of the molecular orbitals. We used split valence basis sets 3-21G, 6-31G, 6-31G+, 6-31G(d), and 6-311G++(2d,p) (where "G" stands for Gaussian type of functions and the integers before G denote the number of primitive exponents involved in the calculations) with added polarization (2d,p) and diffuse functions ("+", "++"). According to our calculations, the additional diffuse functions provide results that are close to those results obtained by means of high level of theory functions, namely, 6-311G++(2d,p). For instance we found that the value of α_{unit} of benzene calculated at a HF/3-21G+ level of theory has only 7% deviation from the value obtained by the more sophisticated HF/6-311G++(2d,p) level but requires 46 times less time. In our opinion, the HF/3-21G+ gives adequate results in a reasonable amount of time and can be used for both the geometry optimization and single point property calculations. Details concerning the used quantum chemical calculations can be found elsewhere.²⁶⁻²⁸

As seen in Table IV it gives a good agreement with experimentally observed refractive indices (cf. Table II). The reason that the calculated refractive indices of PPQ2b and PPQ3 are lower than their measured refractive indices, is the uncertainty of the calculation method (recommended density functional theory (DFT) method with a large basis set [as a

B3LYP/311G++(2*d*,*p*)] required an inadequately long period of time for a single point calculation, ca. 6 months. The current method HF/3-21G+ needs approximately 24–28 h for a single point calculation on a 2 GHz computer using GAUSSIAN 98 software. The procedure for the geometrical optimization of the molecular structure (potential energy minimization) is performed first with the semiempirical method AM1. The following optimizations are made by HF/3-21G+ which is also used for polarizability calculations. The macroscopic properties of the material are determined by the geometry of the polymeric chains averaging over the polarizability tensor of the repeated unit. Usually one assumes a Gaussian coil conformation of the polymeric chain in the solid providing a random averaging over the molecular anisotropy of polarizability. This leads to isotropic optical properties in the amorphous polymeric solid. We therefore assumed that the chain repeat units have random oriented vicinity on the microscopic level. That allows us to apply the Lorentz field approximation. However, taking into account the macroscopic medium, the ensemble of polymer chain units can have a slight orientation due to flow alignment during spin coating and this forms a basis for the observed birefringence.

By differentiating in Eq. (6) P with respect to n one can easily obtain a formula giving an upper limit of birefringence for these materials:

$$\Delta n = \frac{2\pi(n^2 + 2)^2}{9n} \Delta P = \frac{2\pi(n^2 + 2)^2}{9n} \frac{\Delta\alpha_{\text{unit}}}{V_{\text{unit}}}, \quad (11)$$

where $\Delta\alpha_{\text{unit}}$ is the anisotropy of polarizability of the molecular structural unit,

$$\Delta\alpha_{\text{unit}} = \alpha_{xx} - \frac{\alpha_{yy} + \alpha_{zz}}{2}. \quad (12)$$

Equation (12) is a first approximation, where the polymeric unit is represented by a solid cylinder with α_{xx} as polarizability along the long axis. For an isotropic bulk material an averaging takes place and the axis direction distribution is spherical, and hence, no birefringence is prominent. Due to hydrodynamic forces during spin coating, however, the distribution becomes oblate ellipsoid. This leads to the observed birefringence in the spin-coated films where the refractive index for TE modes is higher than that for TM modes. In order to quantify the difference between the experimental value of birefringence Δn_{expt} and the theoretical value Δn_{calc} calculated using Eq. (11) one can introduce the ellipticity parameter γ ,

$$\gamma = 1 - \frac{\Delta n_{\text{expt}}}{\Delta n_{\text{calc}}}. \quad (13)$$

The experimental value of birefringence is given by $\Delta n_{\text{expt}} = n_{\text{TE}}^{\infty} - n_{\text{TM}}^{\infty}$ (see Table III). An ellipticity parameter of zero describes complete orientation of the polymer chains (stretched chains) corresponding to the idealized “cylinder” model of the polymer chain used to derive Eq. (13). A γ value of 1 represents the isotropic case where no birefringence occurs. For PPQ2b $\Delta n_{\text{expt}} = 0.042$ and for PPQ3 $\Delta n_{\text{expt}} = 0.030$ were found. This leads to an ellipticity param-

eter of $\gamma = 0.943$ for both polymers which describes a situation close to complete random packing of the molecular units. This shows that even a small deviation of γ by about 6% from the isotropic behavior, where the ideal ellipticity parameter γ is 1, has a big influence on the values of birefringence as observed in our case.

IV. CONCLUSION

The two investigated polyphenylquinoxalines (PPQs) are well soluble materials, which can be used to prepare thin films of high optical quality by spin-coating, being transparent in the visible and near infrared spectral ranges. They show strong absorption in the ultraviolet and only a very weak tail absorption in the blue spectral range, which gives them a slightly yellow color. The refractive indices reach values around 1.7 in the transparency region, which is considerably higher than the refractive indices of other aromatic polymers such as polystyrene or polycarbonate. The dispersion of refractive index is relatively high as illustrated by an Abbe number of approximately 10. Spin coating causes birefringence in the prepared films where the refractive index for TE modes is higher than that for TM modes. This can be explained by hydrodynamic forces causing a certain chain alignment during spin coating, which is then frozen after drying the films. Theoretical studies show, however, that this birefringence is caused by only a slight deviation from random packing of molecular units. This can be expected because the investigated polymers do not show liquid crystalline behavior where higher birefringence could be inferred by a deposition process from the liquid phase. The low losses obtained in the range of 0.8–0.9 dB/cm and the high thermal stability of the polymer films make the polyphenylquinoxalines interesting candidates for preparation of waveguides for photonic devices.

ACKNOWLEDGMENTS

The authors would like to thank the DFG for the financial support under Contract No. SCHR-642/3-3(4), the University of Applied Sciences Wildau (UASW), Germany, and the Ministry of Science, Technology and Culture of the state of Brandenburg, Germany. The authors would also like to thank Dr. P.W. Schmidt (UASW) for his valuable suggestions during the course of this work.

¹J. M. Augl and H. J. Booth, *J. Polym. Sci., Polym. Chem. Ed.* **11**, 2179 (1973).

²J. R. Murray, J. C. Scott, V. Y. Lee, R. D. Miller, and D. Marsitzky, *Abstr. Pap. - Am. Chem. Soc.* **841**, 0065 (2001).

³M. Jandke, P. Strohhriegl, J. Gmeiner, W. Brutting, and M. Schwoerer, *Synth. Met.* **111–112**, 177 (2000).

⁴B.-S. Kim, J. E. Korleski, Y. Zhang, D. J. Klein, and F. W. Harris, *Polymer* **40**, 4553 (1999).

⁵F. L. Hedberg, F. E. Arnold, and R. F. Kovar, *J. Polym. Sci., Polym. Chem. Ed.* **12**, 1925 (1974).

⁶I. H. Ooi, P. M. Hergenrother, and F. W. Harris, *Polymer* **41**, 5095 (2000).

⁷W. J. Wrasidlo and J. M. Augl, *Polym. Prepr. (Am. Chem. Soc. Div. Polym. Chem.)* **10**, 1353 (1969).

⁸C. Hamciuc, E. Hamciuc, M. Bruma, and N. M. Belomoina, *Eur. Polym. J.* **32**, 837 (1996).

⁹M. Bruma, B. Schulz, T. Kopnick, B. Stiller, and F. Mercer, *Mater. Sci. Eng., C* **8–9**, 361 (1999).

¹⁰J. Bettenhausen, M. Greczmiel, M. Jandke, and P. Strohhriegl, *Synth. Met.*

- 91**, 223 (1997).
- ¹¹C. Fluerau, S. Schrader, V. Zauls, H. Motschmann, B. Stiller, and R. Kiebooms, *Synth. Met.* **111–112**, 603 (2000).
- ¹²S. Schrader, D. Prescher, and V. Zauls, in *Second-Order Organic Non-linear Optics*, edited by M. Eich (Proc. SPIE, San Diego, 1998), pp. 160–171.
- ¹³P. M. Hergenrother and H. H. Levine, *J. Polym. Sci., Part A-1* **5**, 1453 (1967).
- ¹⁴J. K. Stille and J. R. Williamson, *J. Polym. Sci., Part A: Gen. Pap.* **2**, 3867 (1964).
- ¹⁵J. K. Stille and J. R. Williamson, *J. Polym. Sci., Part B: Polym. Lett.* **2**, 209 (1964).
- ¹⁶W. Wrasidlo and J. M. Augl, *J. Polym. Sci., Part B: Polym. Lett.* **7**, 281 (1969).
- ¹⁷W. Wrasidlo and J. M. Augl, *J. Polym. Sci., Part A-1* **7**, 3393 (1969).
- ¹⁸P. K. Tien and R. Ulrich, *J. Opt. Soc. Am.* **60**, 1325 (1970).
- ¹⁹P. K. Tien, R. Ulrich, and R. J. Martin, *Appl. Phys. Lett.* **14**, 291 (1969).
- ²⁰R. Ulrich and R. Torge, *Appl. Opt.* **12**, 2901 (1973).
- ²¹T. Watanabe, H. S. Nalwa, and S. Miyata, in *Nonlinear Properties of Organic Molecules and Polymers*, edited by H. S. Nalwa and S. Miyata (CRC, Boca Raton, 1997), pp. 57–88.
- ²²J. D. Swalen and F. Kajzar, in *Organic Thin Films for Waveguiding Non-linear Optics*, edited by J. D. Swalen and F. Kajzar (Gordon and Breach, Amsterdam, 1996), Vol. 3, p. 12.
- ²³O. Olabisi, *Handbook of Thermoplastics* (Dekker, New York, 1997).
- ²⁴A. A. Askadskii, *Physical Properties of Polymers: Prediction and Control* (Taylor & Francis, Amsterdam, 1996), Vol. 2.
- ²⁵F. Ay, A. Kocabas, C. Kocabas, A. Aydinli, and S. Agan, *J. Appl. Phys.* **96**, 7147 (2004).
- ²⁶P. R. Westmoreland, *Applying Molecular and Materials Modeling* (Springer, New York, 2002).
- ²⁷A. Hinchliffe, *Molecular Modelling for Beginners* (Wiley, New York, 2003).
- ²⁸M. L. Caffery, P. A. Dobosh, and D. M. Richardson, *Laboratory Exercises Using HyperChem* (Hypercube, Gainesville, FL, 1998).